

Mechanically stacked four-junction concentrator solar cells

Myles A. Steiner, John F. Geisz, J. Scott Ward, Iván García, Daniel J. Friedman, Richard R. King, Philip T. Chiu, Ryan M. France, Anna Duda, Waldo J. Olavarria, Michelle Young, Sarah R. Kurtz,

Abstract — Multijunction solar cells can be fabricated by bonding together component cells that are grown separately. Because the component cells are each grown lattice-matched to suitable substrates, this technique allows alloys of different lattice constants to be combined without the structural defects introduced when using metamorphic buffers. Here we present results on the fabrication and performance of four-junction mechanical stacks composed of GaInP/GaAs and GaInAsP/GaInAs tandems, grown on GaAs and InP substrates, respectively. The two tandems were bonded together with a low-index, transparent epoxy that acts as an omni-directional reflector to the GaAs bandedge luminescence, while simultaneously transmitting nearly all of the sub-bandgap light. As determined by electroluminescence measurements and optical modeling, the GaAs subcell demonstrates a higher internal radiative limit and thus higher subcell voltage, compared with GaAs subcells without enhanced internal optics; all four subcells exhibit excellent material quality. The device was fabricated with four contact terminals so that each tandem can be operated at its maximum power point, which raises the cumulative efficiency and decreases spectral sensitivity. Efficiencies exceeding 38% at one-sun have been demonstrated. Eliminating the series resistance is the key challenge for the concentrator cells. We will discuss the performance of one-sun and concentrator versions of the device, and compare the results to recently fabricated monolithic four-junction cells.

Index Terms — III-V solar cell; Mechanical stack; Multijunction solar cell; Photon recycling.

We present results on four-junction, four-terminal solar cells that were fabricated by mechanically stacking separate two-junction monolithic two-terminal tandems. Though requiring two growths and two substrates, the mechanically stacked architecture has several advantages over the more traditional monolithic structures such as the IMM. In the mechanical stack, the various junctions can be grown lattice-matched to a suitable substrate, without the need for a thick, compositionally graded buffer layer to accommodate the lattice mismatch [1]. This enables high material quality in all four junctions. Additionally, each substrate may be chosen to better match the thermal expansion of the epilayers grown on that substrate. The ability to separately contact the two tandems removes the need to current match all four junctions and allows each to be operated at its maximum power point, which should reduce the spectral sensitivity and increase the time-integrated energy yield of the device. Most significantly, the back surface of at least one of the intermediate junctions is readily accessible and can be coated with optical layers that aid the photon management, providing a potential efficiency

boost of 0.5% at one-sun [2]; if reflectors were somehow placed behind every junction, the total efficiency boost could be as high as 2%. The cells described here were bonded together with a low-index, transparent epoxy. Because of the large contrast in the index of refraction, the epoxy acts as an omni-directional reflector to the bandedge luminescence from the GaAs junction [3], which can enhance the photon recycling and therefore the efficiency.

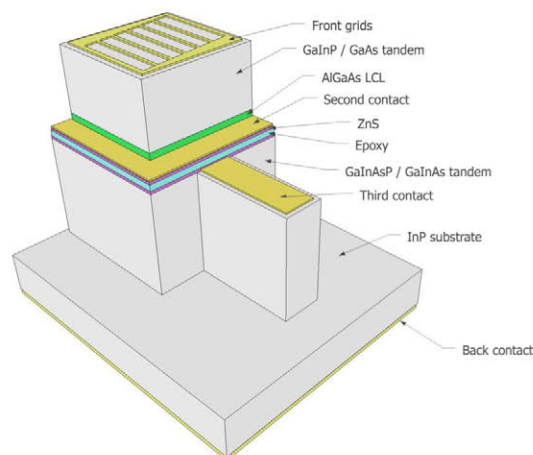


Fig. 1. 3D schematic of the mechanical stack layer structure (not to scale).

The four-junction devices described here consist of an upper GaInP/GaAs (1.85/1.42 eV) tandem grown at NREL and a lower GaInAsP/GaInAs (1.05/0.74 eV) tandem grown at Spectrolab. The upper tandem was grown inverted and the substrate was removed as part of the processing. The lower tandem was grown upright on n-type InP and the substrate remained part of the final structure, though the processing could be adapted to accommodate an inverted lower tandem.

Figure 1 shows a schematic and Fig. 2 shows a composite optical image of the mechanical stack. The upper mesa and front grids are clearly visible in Fig. 2, but other buried features can be weakly discerned. The structure was designed so that the lower tandem would have a larger mesa area than the upper tandem, to accommodate any misalignments during the bonding process. The upper tandem mesa and gridded back contact act as an aperture to the lower tandem and all four junctions have the same 0.1 cm^2 illuminated area. The busbars on the front of the third junction, visible in Fig. 2, are therefore positioned outside the aperture area so that they do not contribute additional shadowing. A long tab extends off

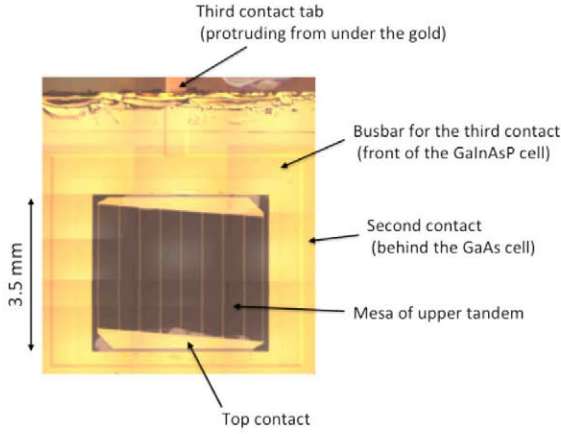


Fig. 2. Nomarski composite image of the mechanically stacked solar cell. Buried features can be seen because the variation in thickness creates visual contrast. The mesa of the upper tandem is aligned with the aperture behind the second junction, and fits well within the busbar of the third junction. External contact to the third junction is made on the protruding tab shown at the top of the image. The fourth contact is made to the back of the n-type InP wafer.

the side of the lower tandem, as shown in Fig. 1, allowing the third contact metal to protrude from beneath the upper tandem for external access. The grids of the first and second contacts are aligned, but the third contact grids are orthogonal to the upper grids and can be discerned in Fig. 2 under close inspection. The fourth contact is made to the back of the n-type InP substrate. Thick, transparent lateral conduction layers were grown behind the GaAs cell (green layer in Fig. 1) and in front of the GaInAsP cell. The two tandems are separated by a low viscosity transparent epoxy with a refractive index of ~ 1.5 (blue layer in Fig. 1), and on either side of the epoxy we deposited 1500 Å ZnS (pink layers in Fig. 1) to increase the transmission of incident light to the lower tandem.

Figure 3 shows the external quantum efficiency (EQE) of a concentrator device. The blue curves are for the GaInP/GaAs tandem and the red curves are for the GaInAsP/GaInAs tandem. Bias light was used to separate the responses of the GaInP and GaAs cells, and of the GaInAsP and GaInAs cells, but because the tandems are not series connected there is no need to over-bias all three non-limiting junctions. Strong luminescent coupling can be observed between the two junctions of each tandem, evidence of the high material quality [4].

Figure 4 shows the one-sun IV curves under conditions equivalent to the G173 direct solar spectrum at 1000 W/m^2 , measured on a class A adjustable solar simulator (uncertified at present). Using calibrated reference cells, the spectrum was adjusted to give the correct photocurrents in each junction, and then the tandems were measured separately. Despite the enhanced reflectance from the epoxy, there remains some luminescent coupling from the GaAs junction to the GaInAsP junction, and care must be taken to bias the upper tandem correctly when measuring the lower tandem [5]. With the upper tandem properly biased at J_{sc} or V_{mp} , rather than V_{oc} , the lower tandem J_{sc} decreases by $\sim 1 \text{ mA/cm}^2$, or about 9%.

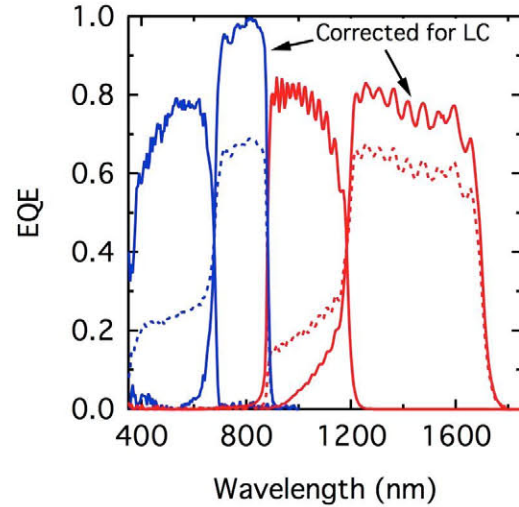


Fig. 3. EQE for a 4J mechanical stack. The dashed lines show the raw data for the second and fourth junctions, showing strong luminescent coupling from the first and third junctions, respectively.

Under these conditions, the cumulative efficiency of the tandem is $28.5\% + 8.91\% = 37.4\%$, which is comparable to the best reported efficiencies for concentrator cells at one-sun. We estimate the uncertainty on the cumulative efficiency to be $\pm 2\%$ (absolute). In our J-PV paper, we will analyze the tradeoff between enhanced photon recycling and luminescent coupling. A similar mechanical stack with a 0.25 cm^2 mesa and a one-sun metallization demonstrated a cumulative efficiency of $38.8 \pm 1.0\%$ under the global spectrum.

Figure 4 also shows the measurement with the second and third contacts shorted to each other, so that the device acts as a two-terminal, four-junction cell. In that case the efficiency drops to $\sim 35.4\%$, largely because the bandgap combination

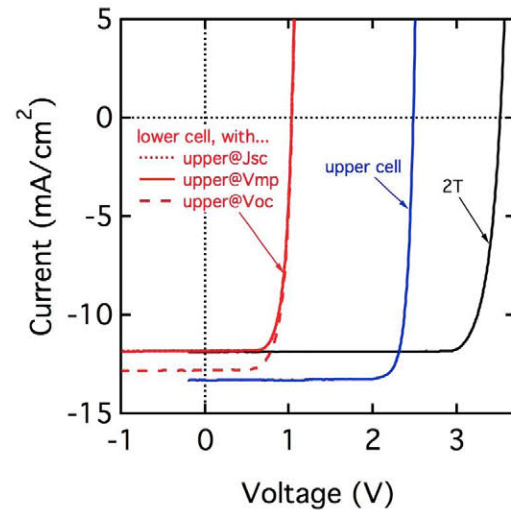


Fig. 4. IV curves on an adjustable solar simulator, under a spectrum equivalent to AM1.5 G173 direct at 1000 W/m^2 . The red curves show the lower tandem under various conditions of upper tandem bias. The cell can be measured as a two-terminal device by shorting the second and third terminals (black curve).

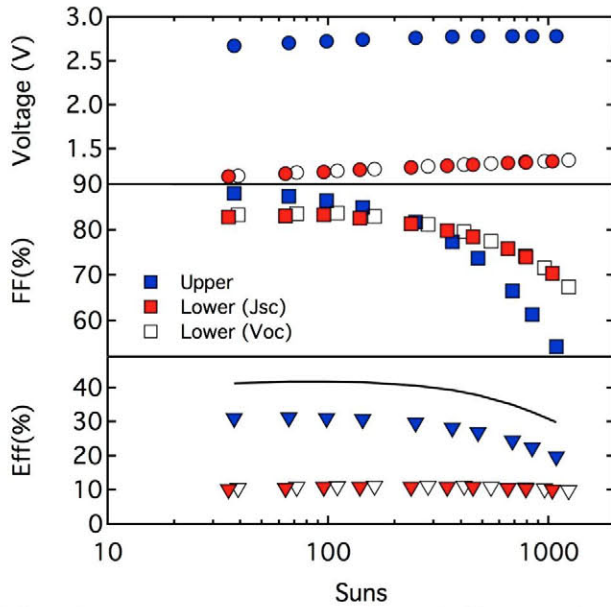


Fig. 5. Concentrator parameters V_{oc} , FF and Eff, measured on the High Intensity Pulsed Solar Simulator (HIPSS). The spectrum was not adjusted. The lower tandem was measured with the upper tandem at short-circuit, to reproduce the appropriate luminescent coupling.

has yielded individual photocurrents that are not all matched. Some of the loss is therefore mitigated by operating the two tandems at their respective maximum power points.

Figure 5 shows the cell's performance under concentration, with the upper tandem biased at J_{sc} during the measurement of the lower tandem. The data were acquired on a HIPSS pulsed solar simulator. The fill factors and efficiencies are over-estimated because this simulator does not allow for the spectrum to be adjusted correctly for all four junctions, but the trends are accurate to characterize the series resistance problems; NREL official measurements with a spectrally adjustable simulator will be reported at the conference. The FF decreases steadily for both tandems, indicating excessive series resistance. For the upper tandem, the source is likely the contact resistance at the front of the cell. For the lower tandem, the source is more likely within the tunnel junction layers. We are working to remedy both issues. The smooth, logarithmic increase in V_{oc} indicates that there are no heating artifacts at the concentrations studied. The maximum cumulative efficiency of this preliminary device is $\sim 42\%$ at ~ 40 suns.

With modifications to the cells over the next few months, we expect to achieve peak cumulative efficiencies $> 45\%$ at elevated concentration. We will discuss the electroluminescence measurements of these cells and compare them to similar measurements on recent 4J-IMM cells. The data (not shown) clearly indicate an improvement of the material quality of the lattice-matched GaInAsP and GaInAs lattice-matched junctions compared to the corresponding, mismatched junctions in the IMM, and also show that the internal radiative limit of the second junction has increased due to the enhanced photon recycling.

ACKNOWLEDGMENTS

The authors are pleased to thank Prof. Eli Yablonovitch for useful and inspiring conversations. Research was supported by the U.S. Department of Energy under Contract no. DE-AC36-08GO28308 with the National Renewable Energy Laboratory.

REFERENCES

- [1] R. M. France, J. F. Geisz, M. A. Steiner, I. García, W. E. McMahon, and D. J. Friedman, "Quadruple junction inverted metamorphic concentrator devices," *IEEE Journal of Photovoltaics*, vol. 5, p. 432, 2015.
- [2] M. A. Steiner, J. F. Geisz, I. Garcia, D. J. Friedman, A. Duda, and S. R. Kurtz, "Optical enhancement of V_{oc} in high quality GaAs solar cells," *J. Appl. Phys.*, vol. 113, pp. 123109-1 - 123109-11, 2013.
- [3] V. Ganapati, C.-S. Ho, and E. Yablonovitch, "Intermediate mirrors to reach theoretical efficiency limits of multi-bandgap solar cells," *IEEE Journal of Photovoltaics*, vol. 5, p. 410, 2014.
- [4] M. A. Steiner, J. F. Geisz, I. Garcia, D. J. Friedman, A. Duda, W. J. Olavarria, *et al.*, "Effects of Internal Luminescence and Internal Optics on V_{oc} and J_{sc} of III-V Solar Cells," *IEEE Journal of Photovoltaics*, vol. 3, pp. 1437-1442, 2013.
- [5] M. A. Steiner, M. W. Wanlass, J. J. Carapella, A. Duda, J. S. Ward, T. E. Moriarty, *et al.*, "A Monolithic Three-Terminal GaInAsP/GaInAs Tandem Solar Cell," *Progress in Photovoltaics*, vol. 17, pp. 587-593, Dec 2009.